

Contents lists available at ScienceDirect

Petroleum Science

journal homepage: www.keaipublishing.com/en/journals/petroleum-science



Original Paper

Improving the anti-collapse performance of water-based drilling fluids of Xinjiang Oilfield using hydrophobically modified silica nanoparticles with cationic surfactants



He Li ^{a, b}, Xian-Bin Huang ^{a, b, *}, Jin-Sheng Sun ^{a, b}, Kai-He Lv ^{a, b}, Xu Meng ^{a, b}, Zhen Zhang ^c

- ^a Key Laboratory of Unconventional Oil & Gas Development (China University of Petroleum (East China)), Ministry of Education, Qingdao, 266580, Shandong, PR China
- ^b School of Petroleum Engineering, China University of Petroleum (East China), Qingdao, 266580, Shandong, PR China
- ^c PetroChina Tarim Oilfield Company, Korla, 841000, Xinjiang, PR China

ARTICLE INFO

Article history: Received 10 May 2022 Received in revised form 22 October 2022 Accepted 30 October 2022 Available online 2 November 2022

Edited by Yan-Hua Sun

Keywords: Hydrophobic nanoparticle Wetting alteration Wellbore stability Water-based drilling fluids Shale

ABSTRACT

Wellbore instability, especially drilling with water-based drilling fluids (WBDFs) in complex shale formations, is a critical challenge for oil and gas development. The purpose of this paper is to study the feasibility of using hydrophobically modified silica nanoparticle (HMN) to enhance the comprehensive performance of WBDFs in the Xinjiang Oilfield, especially the anti-collapse performance. The effect of HMN on the overall performance of WBDFs in the Xinjiang Oilfield, including inhibition, plugging, lubricity, rheology, and filtration loss, was studied with a series of experiments. The mechanism of HMN action was studied by analyzing the changes of shale surface structure and chemical groups, wettability, and capillary force. The experimental results showed that HMN could improve the performance of WBDFs in the Xinjiang Oilfield to inhibit the hydration swelling and dispersion of shale. The plugging and lubrication performance of the WBDFs in the Xinjiang Oilfield were also enhanced with HMN based on the experimental results, HMN had less impact on the rheological and filtration performance of the WBDFs in the Xinjiang Oilfield. In addition, HMN significantly prevented the decrease of shale strength. The potential mechanism of HMN was as follows. The chemical composition and structure of the shale surface were altered due to the adsorption of HMN driven by electrostatic attraction. Changes of the shale surface resulted in significant wettability transition. The capillary force of the shale was converted from a driving force of water into the interior to a resistance. In summary, hydrophobic nanoparticles presented a favorable application potential for WBDFs.

© 2023 The Authors. Publishing services by Elsevier B.V. on behalf of KeAi Communications Co. Ltd. This is an open access article under the CC BY-NC-ND license (http://creativecommons.org/licenses/by-nc-nd/4.0/).

1. Introduction

Wellbore instability in complex shale formations has been a huge engineering and technical problem for a long time, especially in horizontal drilling with water-based drilling fluids (WBDFs). Wellbore instability problems, such as borehole collapse, bit balling, and stuck pipe, severely restrict the efficient production of oil and gas. Shale in complex formations is highly sensitive to water due to its rich clay content. When the shale interacts with water

E-mail address: 20170092@upc.edu.cn (X.-B. Huang).

from WBDFs, the shale undergoes hydration dispersion and swelling, resulting in a continuous reduction in wellbore strength (Lei et al., 2020). Under the action of pressure difference, the wellbore instability occurs.

In response to wellbore instability, various types of inhibitors were added to the WBDFs to inhibit shale hydration. Inorganic salts, such as potassium chloride, sodium chloride, and ammonium chloride, were common clay stabilizers, which controlled clay swelling mainly through ion exchange and low hydration energy (Parizad and Shahbazi, 2016; Young and Smith, 2000). However, very high concentrations of salts (5–10 wt%) were required to obtain good inhibition, which caused clay flocculation with a high filtration loss (Ma et al., 2017; Zhong et al., 2016). Organic salts, represented by formates (HCOOK), were also effective shale

^{*} Corresponding author. Key Laboratory of Unconventional Oil & Gas Development (China University of Petroleum (East China)), Ministry of Education, Qingdao, 266580, Shandong, PR China.

inhibitors, which inhibit shale hydration through ion exchange and reduction of drilling fluid water activity (Chu et al., 2020; Gholami et al., 2018; Guancheng et al., 2016a). However, the high addition of organic salts (≥5 wt%) to the drilling fluid resulted in higher costs (Davarpanah and Mirshekari, 2019; Gao, 2019). Despite the high dosage, the inhibition still could not meet the demand in complex formations. Then, encapsulated polymers, such as partially hydrolyzed polyacrylamide, prevent the decomposition of shale by adsorbing at multiple sites on the rock surface (Gholami et al., 2018; Yang et al., 2017). Encapsulated polymers caused a dramatic increase in drilling fluid viscosity due to their high molecular weight. The action mechanism of encapsulated polymers resulted in a limited inhibition effect, as it could not inhibit the entry of water into the clay layer (Suter et al., 2011). The lack of inhibition and resulting high viscosity limited the application of encapsulated polymers (Jiang et al., 2018). In addition, amine-based shale inhibitors, mainly oligocationic amines (polyether amines, polyethylene amine salts, and ether amines), had attracted particular attention from researchers due to their unique inhibition performance in recent years (Peng et al., 2013; Zhong et al., 2015). The main action mechanism was to inhibit the clay swelling by inserting into the interlayer of clay, and the positively charged groups neutralized the negative charge of clay to reduce the hydration repulsion of clay (Bai et al., 2017; Guancheng et al., 2016). Despite the good inhibition performance shown by amine-based inhibitors, the problem of shale hydration remained unresolved under complex conditions. Existing inhibitors were still insufficient to meet the need for safe and efficient oil and gas extraction.

For hydrophilic shale, it is easy to interact with water of drilling fluid to cause hydration due to its hydrophilic properties. It was shown that changing the rock wettability can improve wellbore stability (Ni et al., 2019; Yue et al., 2018). Therefore, the development of a new WBDF additive, which could alter the rock wettability to reduce shale-water interaction, was a promising method to improve wellbore stability. Nanoparticles have features of small size, large specific surface area, high adsorption capacity, and high surface reactivity. Reports had shown that nanoparticles could improve the rheology, inhibition, and lubricity of drilling fluids (Ibrahim and Saleh, 2020). It had also been shown that nanoparticles could stabilize shale by reducing filtrate intrusion through physical plugging of shale pores (Rivet, 2009). In addition, many studies had also been conducted to alter the wettability of rocks with nanoparticles (Sheshdeh, 2015). However, the existing studies of altering rock wettability with nanoparticles were mostly focused on enhancing oil recovery (EOR) (Al-Anssari et al., 2016). It mainly employed hydrophilic nanoparticles to convert reservoir rocks from lipophilic to hydrophilic to improve oil drive efficiency. Less attention had been devoted to the study of altering the wellbore rock wettability to improve wellbore stability with hydrophobically modified nanoparticles. Hydrophobic surfaces can be formed in two ways, either by creating a microscopic rough structure on a low surface energy surface or by modifying the rough surface using a low surface energy chemical agent (Ni et al., 2019). Low-surfaceenergy surfactants were used to modify inexpensive silica nanoparticles to prepare hydrophobically modified nanoparticles (HMN) in this paper. The physicochemical interaction of the rock with water was inhibited by converting the wellbore rock from hydrophilic to hydrophobic, combined with the plugging effect of nanoparticles.

In this paper, a simple method for the hydrophobic modification of nanoparticles was provided. Horizontal wells were more concentrated in Xinjiang Oilfield and prone to collapse during drilling. A typical WBDF used in the Xinjiang Oilfield was chosen as the experimental object. The effect of HMN as a shale stabilizer on the comprehensive performance of the WBDF used in Xinjiang

Oilfield, including inhibition, plugging, rheology, filtration, and lubricity, was evaluated. The experimental evaluation temperature was determined based on the formation temperature in the Xinjiang Oilfield. The drilling depth was generally less than 4500 m, and the downhole temperature was less than 90 °C. In addition, the action mechanism of HMN was analyzed by micromorphological analysis, Fourier transform infrared (FTIR) spectroscopy analysis, wettability measurements, and glass capillary tube rise tests.

2. Materials and methods

2.1. Materials

Hydrophilic fumed silica nanoparticles (30 nm, 99.8 wt%) and potassium bromide (KBr, 99.5 wt%) were purchased from Aladdin Chemical Reagent Co., Ltd (Shanghai, China). The octyl decyl dimethyl ammonium chloride (ODAC, 80 wt%) and methylene blue (98 wt%) were obtained from Macklin Biochemical Co., Ltd. (Shanghai, China). Glass capillary tubes (inner diameter 1.0 mm) were purchased from Qiancheng Analytical Instruments Co. (Jinan, China). Quartz sands (80–100 mesh) were obtained from Lingwei Chemical Co. (Jinan, China). Bentonite, shale samples, and treatment agents for formulating WBDFs of the Xinjiang Oilfield were supplied by the Xinjiang Oilfield Company (China). The detailed mineralogical composition of shale was shown in Table 1.

2.2. Synthesis of HMN

The surface modification of silica nanoparticles was based on previous study (Ma et al., 2010). Firstly, 5 g of silica nanoparticles were added to 100 mL of deionized water under stirring, followed by ultrasonication of the solution for 20 min to disperse the nanoparticles uniformly. The silica solution was poured into a three-neck flask. Then the temperature was increased to 75 °C in a water bath and 7.5 g ODAC was added to the solution while maintaining vigorous stirring. The reaction was completed after 4 h. Finally, the white powdered product was obtained by drying the solution at 105 °C. The schematic diagram of the reaction mechanism of HMN is shown in Fig. 1.

2.3. Characterization of HMN

A Zetasizer Nano ZS (Malvern Instruments Ltd.; UK) was used for analyzing particle size distribution and charged properties of HMN. Scanning Electron Microscopy (SEM, Nova NanoSEM 450, USA) was performed to observe the surface morphology of HMN. The chemical structure of HMN was examined by a Fourier Transform Infrared Spectrometer (IRTRacer-100, SHIMADZU, Japan).

Table 1Mineralogical composition of shale.

Component	Content, wt%
Quartz	34.7
Potassium feldspar	1.5
Plagioclase	23.1
Siderite	1.2
Calcite	2.4
Halite	2.0
Kaolinite	8.1
Chlorite	2.8
Illite	13.0
Illite/smectite mixed layer	11.2

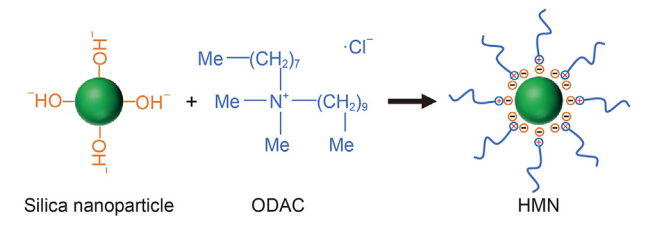


Fig. 1. The schematic diagram of the reaction mechanism of HMN.

2.4. Effect of HMN on comprehensive performance of WBDFs

2.4.1. Formulation of WBDFs in Xinjiang Oilfield

The base mud was prepared by mixing 40.0 g bentonite and 3.0 g sodium carbonate into 1000.0 mL fresh water and leaving it for 16 h at room temperature. The WBDFs of the Xinjiang Oilfield were prepared by mixing each additive with the base mud for 30 min using a mixer at 8000 rpm (Tongchun, Qingdao). The organosilica lignite (HY-2) and polyacrylamide potassium salt (SP-8) were used to control the filtration loss of the WBDFs. The viscosity of the WBDFs in the Xinjiang Oilfield was enhanced using the viscosifier of amphoteric polymer (PMHA-2). The inhibition performance of the system was improved by inorganic salts (potassium chloride), organic salts and amine-based inhibitors. Ultra-fine calcium carbonate was applied as a plugging agent to improve the plugging performance of the WBDFs. The WBDFs lubricity was improved using emulsified asphalt. The pH of the WBDFs was maintained at 9.0 using sodium hydroxide, and the density of WBDFs was adjusted to 1.3 g/cm³ by adding the weighting additive of formate. The detailed composition of WBDFs in the Xinjiang Oilfield was shown in Table 2.

2.4.2. Effect of HMN on inhibition performance of WBDFs

The inhibition performance of WBDFs in the Xinjiang Oilfield was evaluated by bentonite linear swelling tests and shale cutting hot-rolling recovery tests. Both experiments were practical methods to evaluate the inhibition performance. The linear swelling tests were conducted according to the following steps. First, 10 g of bentonite was poured into a pressure tank, which was compacted at a pressure of 10 MPa for 5 min to obtain a cylindrical sample. Next, the obtained samples were placed into test cylinders, which were installed in the CPZ-2 dual-channel linear swelling instrument (Qingdao Tongchun, China). The test WBDFs were added, and the bentonite sample subsequently swelled in the test cylinders. The rate of swelling with time was recorded by computer.

The hot-rolling recovery tests were used to evaluate the performance of WBDFs in the Xinjiang Oilfield to inhibit the hydration and dispersion of shale cuttings. 20 g of shale cuttings between 6

and 10 mesh (1.68–2.81 mm) were added into an aging tank containing 350 mL of WBDFs. The aging tanks were then rolled in a GW-300 roller oven (Qingdao Tongchun, China) for 16 h at 90 $^{\circ}$ C. The shale cuttings were rinsed in a sink with running water after heating. The remaining shale cuttings were sieved using a 40-mesh sieve and weighed after drying to a constant weight. The hotrolling recovery rate was the weight percentage of recovered residual cuttings to the initial cuttings.

2.4.3. Effect of HMN on plugging performance of WBDFs

Sand bed plugging experiments were used to evaluate the plugging performance of WBDFs in the Xinjiang Oilfield. The prepared WBDFs were aged in a roller oven at 90 °C for 16 h. 300 cm³ of quartz sand with 80–100 mesh was evenly spread and compacted in the cylinder of the sand bed filter loss meter (FA, Meike, China), followed by adding of 250 mL of aged drilling fluids. The cylinder of the sand bed filter loss meter was pressurized to 0.7 MPa after closure. The depth of the WBDF intrusion into the sand bed was measured after 30 min at room temperature.

2.4.4. Effect of HMN on rheology, filtration, and lubrication performance of WBDFs

HMN was added to the prepared WBDFs of the Xinjiang Oilfield and stirred at 8000 rpm for 30 min to mix completely. Subsequently, the rheological properties of the WBDFs were measured using a rotational viscometer ZNN-D6 (Qingdao Tongchun Petroleum Co. Ltd, China) according to American Petroleum Institute (API) standards. The rheological parameters, including apparent viscosity (AV), plastic viscosity (PV), yield point (YP), and initial and final shear (G' and G''), were then determined.

The filtration loss performance of WBDFs in the Xinjiang Oilfield was measured according to API standards (API recommended practice 13B-1, 1997). The low temperature and low pressure (LTLP) filtration measurements were carried out using the LPLT filter press at a pressure of 100 psi and ambient temperature. Similarly, high temperature and high pressure (HTHP) filtration losses were measured with an HTHP filter press at a differential pressure of 500 psi and 90 °C.

EP-2 extreme pressure and lubricity tester (Meike, China) was used to evaluate the difference of lubricity performance of WBDFs in the Xinjiang Oilfield before and after the addition of HMN. The lubricator was calibrated using deionized water before the test. The WBDFs were poured into the test cup and placed in the lubricator bracket while keeping the test metal ring below the fluid level. The lubricator was then loaded to 16.95 N·m (150 in-lbs) using a torque wrench. The results were recorded after the instrument had been running for 5 min.

Table 2Composition of the WBDFs used in Xinjiang Oilfield.

Additives type	Additive name	Concentration, wt%	Lab unit, per 400 cm ³ 270.9 cm ³	
Base fluid	Tap water	52.1		
Clay	Bentonite	2.1	10.92 g	
pH regulator	Sodium hydroxide	0.2	1.04 g	
Filtration reducer 1	Organosilicon lignite	0.5	2.6 g	
Filtration reducer 2	Polyacrylamide potassium salt	0.4	2.1 g	
Viscosifier	Amphoteric polymer	0.4	2.1 g	
Inorganic salt	Potassium chloride	3.6	18.7 g	
Organic salt	Formate	5.2	27.0 g	
Shale inhibitor	Polyamine	0.3	1.6 g	
Plugging agent	Ultra-fine calcium carbonate	0.5	2.6 g	
Lubricant	Emulsified asphalt	0.5	2.6 g	
Weighting additive	Carboxylate	34.2	177.8 g	

2.5. Shale strength measurements

Uniaxial compressive strength tests were performed to evaluate shale stability. Shale core columns were dried at a constant weight at 70 °C for 7 d using a vacuum drying oven before the test. The shale core columns were then placed in aging tanks to which 350 mL of WBDFs were added. The aging tanks were then heated at 90 °C for 3 d. Next, the shale core columns were removed and cleaned with tap water. The surface water was removed by drying under ambient conditions. A pressure testing machine (YAW-3000, Chenda test machine Corporation, China) was used for testing the uniaxial compressive strength of the water-bearing shale core columns.

2.6. Mechanism analysis

2.6.1. Micromorphological analysis

The topography of the shale samples before and after treatment was observed by atomic force microscopy (AFM) (Bruker Dimension Icon, Germany) and Scanning electron microscopy (SEM) (Nova NanoSEM 450, USA). The samples polished by Ar ions were prepared by immersion in 2 wt% HMN aqueous solution in aging tanks aged at 90 $^{\circ}\text{C}$ for 16 h. The modified surface was scanned by the force between the probe and the sample surface atoms using the tap method.

2.6.2. FTIR analysis

Fourier transform infrared spectrometer (IRTRacer-100, SHI-MADZU, Japan) was employed to analyze the changes of shale molecular structure and chemical groups after HMN adsorption. The crushed shale samples were first aged in an aqueous solution containing 2 wt% HMN at 90 °C for 16 h. The suspensions were then centrifuged at 6000 rpm for 5 min. The shale samples were dried, and the IR spectra were measured using a KBr pellet method.

2.6.3. Wettability measurements

Shale sheets with a diameter of 2.5 cm were placed in an aging tank containing 350 mL of WBDFs in the Xinjiang Oilfield, and the aging tank was then heated at 90 °C for 16 h using a roller oven. The shale sheets were removed and dried at ambient temperature after cooling. The water contact angle of the shale sheets was tested using an OCA 25 contact angle measuring instrument (Data Physics, Germany) based on the sessile drop method.

2.6.4. Glass capillary tube rise tests

Glass capillary tube rise tests were performed to study the inversion of shale capillary forces on water action after HMN adsorption. The experimental steps were as follows (Feng et al., 2012). First, the glass capillary tubes were rinsed with deionized water and dried in an oven. The dried capillary tubes were aged in different solutions (water, 1 wt% HMN, 2 wt% HMN, 3 wt% HMN) at 90 °C for 16 h. Next, the capillary tubes were purged with highpressure nitrogen and dried in an oven to remove residual liquid. Finally, the capillary tubes were inserted vertically into a waterfilled evaporation dish. The liquid would rise to a certain height along the capillary tube under the action of capillary force. The capillary tubes were taken out after stabilization and the rise height was recorded. The height above the water surface was positive and the height below the water surface was negative. In the present experiment, the glass capillary tubes with the inner diameter of 1 mm were used. The water was stained with methylene blue to facilitate the observation of the capillary tube rise height.

3. Results and discussion

3.1. Characterization of HMN

The FT-IR spectra of silica nanoparticles before and after modification are shown in Fig. 2. For the FT-IR spectra of silica nanoparticles before modification, the wide absorption band found at 3424 cm⁻¹ corresponded to the stretching vibration of the hydroxyl group. A characteristic peak of silica nanoparticles was found at 1104 cm⁻¹, which was attributed to the antisymmetric stretching vibration of the Si–O–Si. The typical absorption peak at 470 cm⁻¹ was caused by the bending vibration of the Si–O in the silica nanoparticles (Kim et al., 2009). After modification, distinct characteristic peaks were found at 2917 and 2850 cm⁻¹, corresponding to the stretching vibration of -CH₂ and -CH₃ in the ODAC, respectively (Ma et al., 2010). In addition, the absorption peak found at 1469 cm⁻¹ was caused by the C–H bending vibration in the ODAC. These characteristic peaks indicated the successful preparation of HMN.

The charged properties of HMN were measured by zeta potential tests. The results are shown in Fig. 3a. The zeta potential of HMN gradually increased with the concentration of HMN. The zeta potentials were 31.0, 35.7, and 36.0 mV when the HMN concentrations were 1.0 wt%, 2.0 wt% and 3.0 wt%, respectively. The positive charge of HMN was ascribed to the quaternary ammonium group of the surfactant, which made it more readily available for electrostatic adsorption with negatively charged clays and rocks.

Fig. 3b demonstrates the variation of particle size of HMN in water with concentration. The maximum particle size of HMN was 220 nm, and the minimum was 68.1 nm. The average particle size was 109 nm at the concentration of HMN of 1.0 wt%. The particle size varied insignificantly when the concentration of HMN in water increased, as shown in Fig. 3b. The microscopic morphological changes of silica nanoparticles before and after hydrophobic modification are shown in Fig. 4a and b, respectively.

3.2. Effect of HMN on comprehensive performance of WBDFs

3.2.1. Effect of HMN on inhibition performance of WBDFs Linear swelling results of bentonite are shown in Fig. 5a. As can

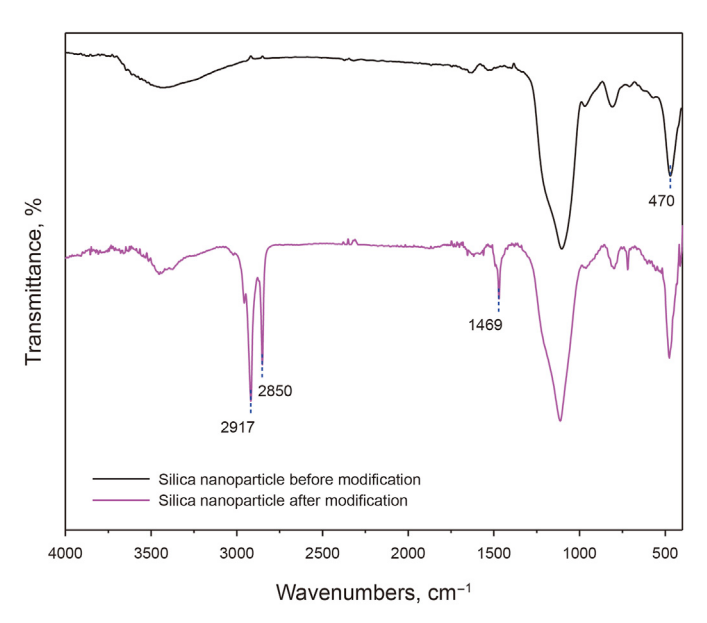
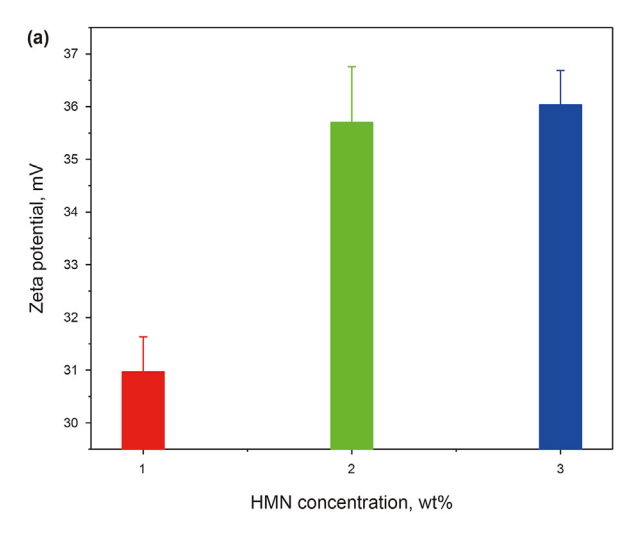


Fig. 2. FT-IR spectra of silica nanoparticles before and after modification with ODAC.



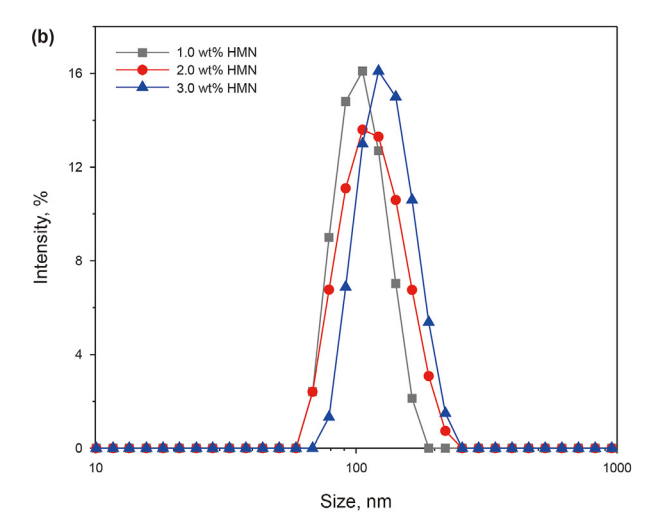


Fig. 3. The effect of HMN concentration on its zeta potential (a) and particle size distribution (b).

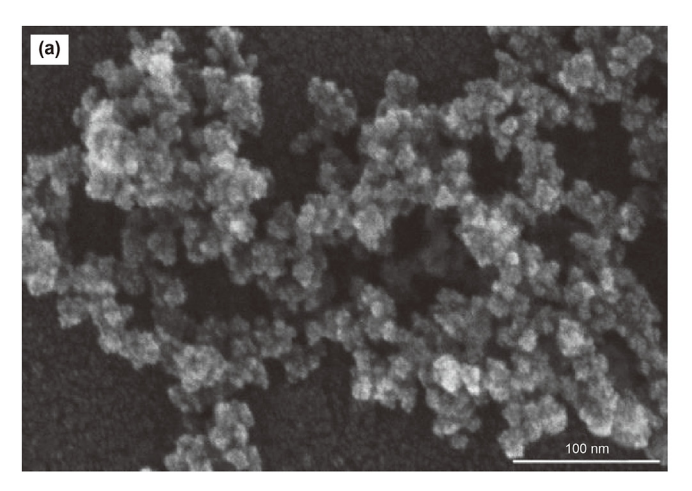
be seen from the graph, despite a slight downward trend in the swelling rate of bentonite, it still swelled rapidly in water in general and eventually reached a high swelling rate (56.2%). The phenomenon was attributed to the unimpeded entry of water molecules into the clay layer, resulting in its hydration and swelling. The swelling rate of bentonite finally reached 41.5% after soaking in 0.5 wt% polyamine solution for 16 h. In contrast, 0.5 wt% HMN resulted in a final swelling rate of 37.2% for the bentonite, which was superior to polyamine. Clays swelled slowly under the action of various inhibitors in the WBDFs of the Xinjiang Oilfield and eventually reached 9.1%. These actions included encapsulation and intercalation of polymer inhibitors and lattice substitution by inorganic salts. It was notable that the inhibition of the original WBDFs of the Xinjiang Oilfield further improved with increasing HMN content (1.0 wt%, 2.0 wt%, and 3.0 wt%), as demonstrated by the extremely low bentonite swelling rate (6.1%, 4.2%, and 2.6%). The swelling rate of the WBDFs in the Xinjiang Oilfield with the addition of 3.0 wt% HMN was less than one-third of that without HMN addition. Moreover, the swelling rate of the clay in the WBDFs added with HMN remained stable more quickly and was maintained at an extremely low level. As mentioned above, HMN improved the ability of WBDFs in the Xinjiang Oilfield to inhibit clay hydration swelling effectively.

The recovery rates of shale cuttings in WBDFs of the Xinjiang

Oilfield with HMN concentration at 90 °C for 16 h are shown in Fig. 5b. The high recovery rate of shale cuttings indicated a better inhibiting effect of WBDFs in the Xinjiang Oilfield on hydration dispersion. The recovery rate of cuttings in water was only 6.6 wt%, which indicated extreme susceptibility to hydration. The recovery rate of shale cuttings in 0.5 wt% polyamine solution was 39.6 wt%. And for HMN, the recovery rate of shale cuttings reached 45.3 wt% in 0.5 wt% HMN solution. It can be seen from Fig. 5b that the recovery of shale cuttings in the original WBDFs of the Xinjiang Oilfield was 73.3 wt% after aging at 90 °C. The shale cuttings recovery improved with increasing HMN content. The recovery increased to more than 80 wt% with the addition of 2.0 wt% HMN. First, HMN adsorbed on the rock cuttings surface by electrostatic attraction. Second, HMN changed the shale surface and formed a hydrophobic structure. Third, HMN converted the shale from hydrophilic to hydrophobic, which prevented water from entering the interior of the shale. Therefore, HMN enhanced the inhibitory effect of WBDFs on shale hydration dispersion.

3.2.2. Effect of HMN on plugging performance of WBDFs

Enhancing the plugging ability of the WBDFs was a very effective means to improve wellbore stability. Studies demonstrated that nanoparticles enhanced the plugging performance of WBDFs (Cai et al., 2012; Rivet, 2009). The sand bed plugging experiment



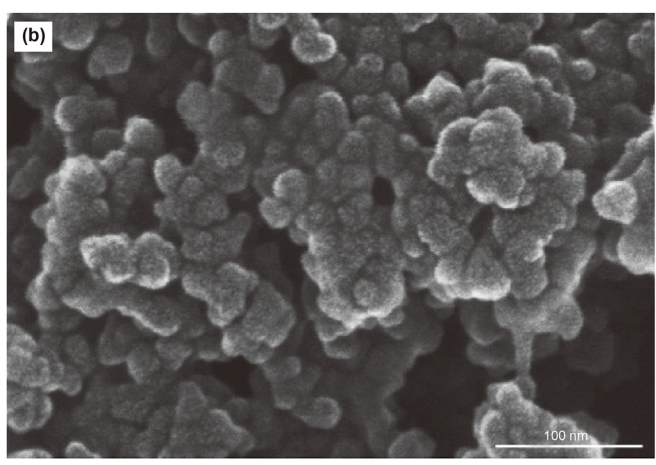
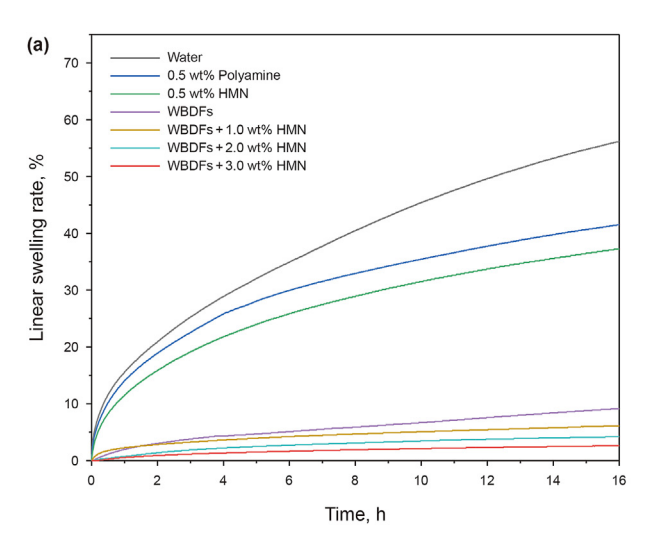


Fig. 4. SEM images of silica nanoparticles before (a) and after (b) modified by HMN.



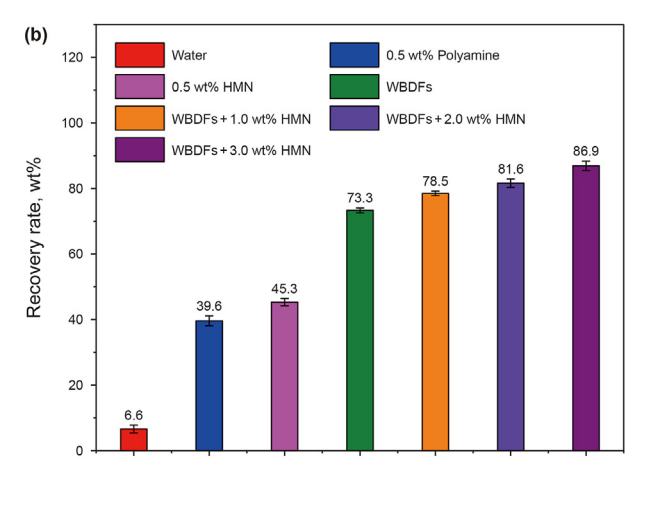


Fig. 5. The results of linear swelling tests (a) and hot-rolling recovery tests (b) for water, inhibitors and WBDFs with different HMN concentrations.

was used to evaluate the plugging properties of the WBDFs in the Xinjiang Oilfield, and the results are shown in Table 3. The lower the depth of WBDF intrusion into the sand bed, the better the plugging ability of WBDFs. As shown in Table 3, the original WBDFs of the Xinjiang Oilfield intruded the sand bed to a depth of 3.0 cm. Due to the addition of HMN, the plugging capacity of the WBDFs in the Xinjiang Oilfield was improved, and the sand bed intrusion height was reduced to 2.4 cm at 3.0 wt% HMN concentration. However, the enhancement of WBDFs in the Xinjiang Oilfield plugging performance by HMN was relatively weak due to the small particle size of HMN.

3.2.3. Effect of HMN on rheology, filtration, and lubrication performance of WBDFs

The effects of increasing concentrations of HMN on the rheological and filtration properties of WBDFs in the Xinjiang Oilfield before and after aging are shown in Fig. 6 and Table 4. Fig. 6a showed that the apparent viscosity of the WBDFs tended to increase with increasing HMN content. The plastic viscosity of the WBDFs presented a similar trend to the apparent viscosity both before and after aging, as shown in Fig. 6b. Although both the apparent viscosity and plastic viscosity of the WBDFs increased, the lesser increase had little effect on the rheological properties of the original WBDFs. In addition, the addition of HMN induced a proper enhancement of the WBDFs yield point, as shown in Fig. 6c. High content of the inferior solid phase (mostly micro and nano particles) in the drilling fluid system increased the viscosity and yield point of the drilling fluid, which was consistent with the findings of

this paper (Saleh and Ibrahim, 2019). HMN were nanoparticles, and its addition increased the number of drilling fluid particles. The nanoparticles could interact with polymer chains and form a stronger spatial network structure as a result. The change was favorable because an appropriate increase in yield point gave the WBDFs a better ability to carry rock cuttings. Carrying rock cuttings to avoid downhole complications was one of the important functions of WBDFs. As seen in Fig. 6d and Table 4, HMN caused a slightly increased filtration loss of WBDFs, which was attributed to the inhibitory effect of HMN on the clay. Mud cake permeability is an important factor affecting filtration loss of drilling fluids. HMN could inhibit the hydration of clay and increased the particle size of clay, thus affecting the permeability of mud cake. Therefore, HMN had an impact on the filtration loss of the drilling fluid.

To reduce borehole drag and torque on the drill pipe, the lubrication performance of the WBDFs needed to be improved and enhanced. Fig. 7 depicts the effect of HMN concentration on the lubrication factor of the WBDFs in the Xinjiang Oilfield. The lubrication factor of the original WBDFs was 0.17. The frictional resistance of the WBDFs decreased significantly with increasing HMN concentration. The friction factors of WBDFs were reduced by 41% (0.10) and 70.6% (0.05) after adding 2.0 wt% HMN and 3.0 wt% HMN, respectively. When nanoparticles were dispersed in the drilling fluid, nanoparticles could improve the smoothness of the contact surface of the drill string and casing. Nanoparticles dispersed between the drill string and the casing converted sliding friction into rolling friction to increase lubrication (Huang et al., 2021; Saffari et al., 2018). The significant increase in lubricity of WBDFs in the

Table 3The depth of sand bed invasion by WBDFs in the Xinjiang Oilfield with different HMN concentrations.

Category	Experimental results					
HMN concentration, wt% Invasion depth, cm	0 3.0	1.0 2.8	2.0 2.7	3.0 2.4		
Image of invasion depth	3.0 m 250 200	2.80 m 250 m 250 m	27 - 110 - 250 - 250 - 150	300 a. 443		

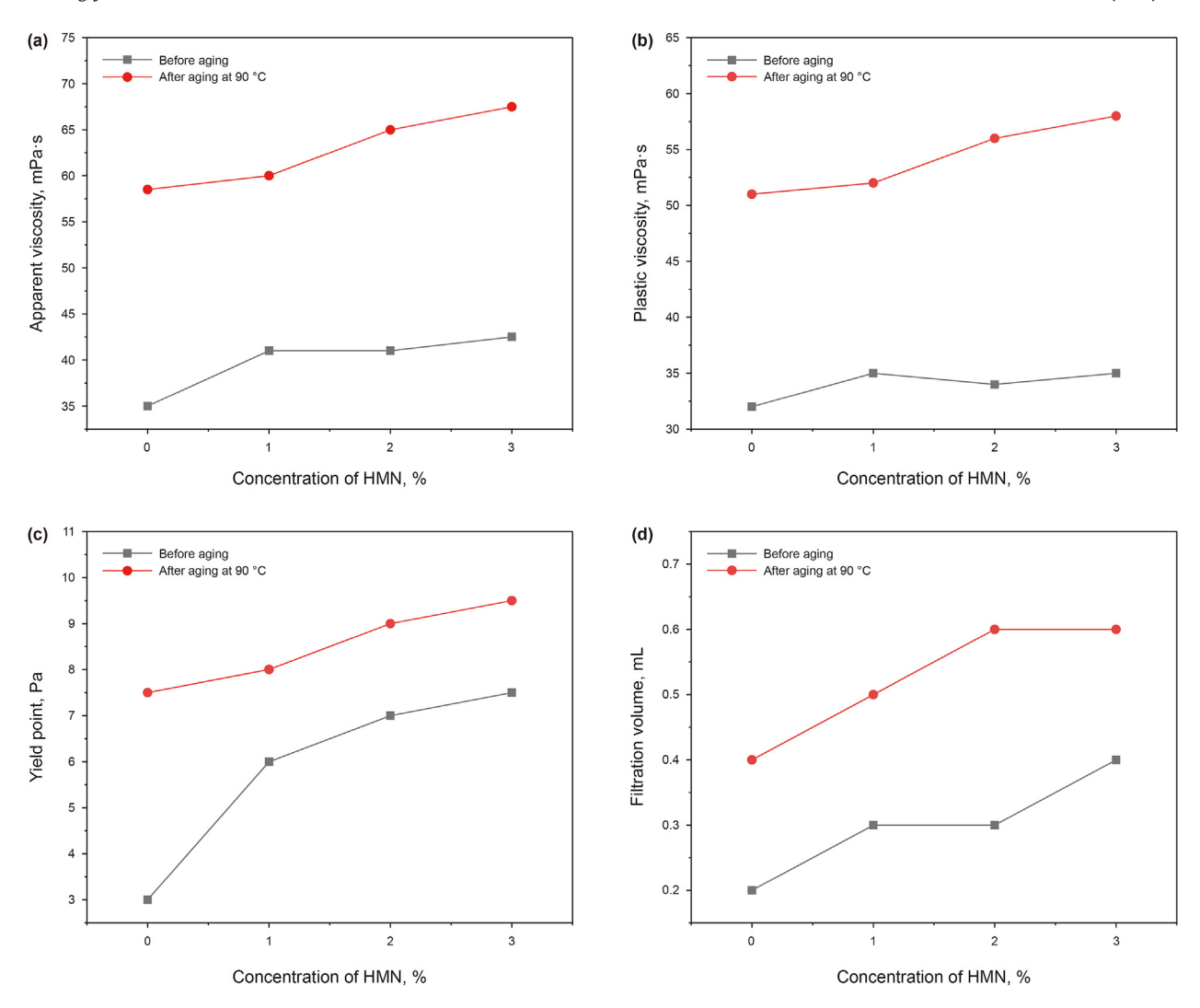


Fig. 6. Effects of HMN on apparent viscosity (a), plastic viscosity (b), yield point (c), and filtration loss (d) of WBDFs in the Xinjiang Oilfield.

Table 4Effect of HMN on rheology and filtration performance of WBDFs in the Xinjiang Oilfield.

Item	T, °C	AV, mPa·s	PV, mPa·s	YP, Pa	<i>G'/G"</i> , Pa	API filtration, mL	HTHP filtration, mL
WBDFs	25	35	32	3	0.5/0.5	0.2	_
	90	58.5	51	7.5	1/2	0.4	7.2
WBDF + 1.0 wt% HMN	25	41	35	6	0.5/1.5	0.3	_
	90	60	52	8	0.5/1	0.5	7.2
WBDF + 2.0 wt% HMN	25	41	34	7	0.5/1.5	0.3	_
	90	65	56	9	3/5	0.6	8.2
WBDF + 3.0 wt% HMN	25	42.5	35	7.5	1.5/2	0.4	_
	90	67.5	58	9.5	6.5/11	0.6	8.4

Xinjiang Oilfield could prevent the occurrence of downhole complications such as stuck drilling. However, it was worth noting that the experimental results only demonstrated that HMN could improve the lubricity between a drill string and a cased wellbore instead of an open-hole wellbore, due to the steel surface of the lubricator.

3.3. Shale strength measurements

The results of the uniaxial compressive strength of shale in WBDFs of the Xinjiang Oilfield with different HMN concentrations

are shown in Fig. 8. The shale had a lower strength limit (82.3 MPa) after heating in the original WBDFs of the Xinjiang Oilfield, which originated from the hydration caused by water entering the shale interior. In contrast, the addition of HMN to the WBDFs resulted in a significant increase in shale strength. The compressive strength of shale in WBDFs with 1.0 wt% HMN and 2.0 wt% HMN was 117.3 and 123.0 MPa, respectively. Moreover, the compressive strength of shale was further enhanced to 137.0 MPa with 3.0 wt% HMN, which was close to the compressive strength of untreated shale (144.6 MPa). This enhancement was derived from the wettability alteration of the shale by HMN, which was confirmed above. The

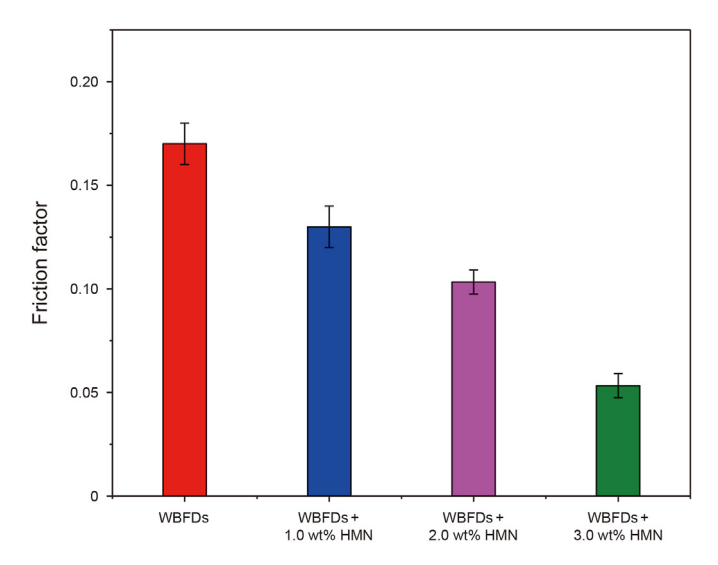


Fig. 7. Friction factors of WBDFs in the Xinjiang Oilfield containing different concentrations of HMN.

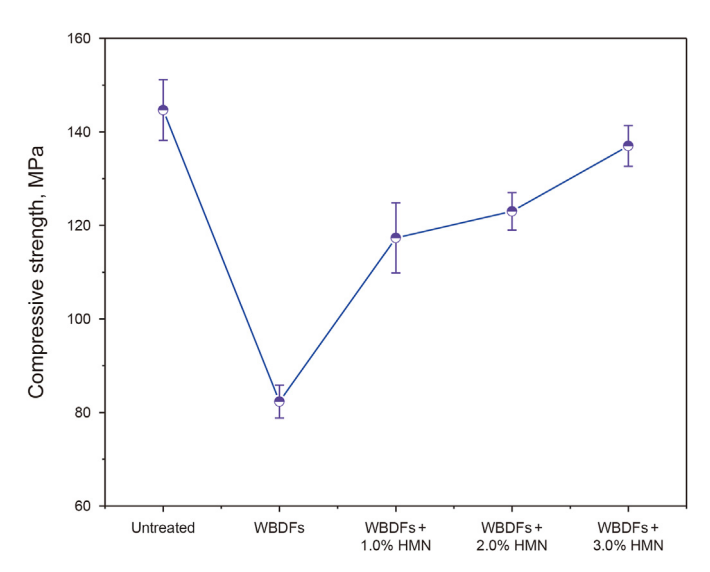


Fig. 8. The uniaxial compressive strength of shale in WBDFs of the Xinjiang Oilfield with different HMN concentrations.

improvement in shale strength indicated that HMN could effectively enhance the anti-collapse performance of WBDFs.

3.4. Mechanism analysis

3.4.1. Micromorphological analysis

SEM images of the shale before and after 2.0 wt% HMN treatment are shown in Fig. 9. The surface of the original shale was uneven and presented a layered structure (see Fig. 9a). As for the treated shale, it was obvious from Fig. 9b that numerous nanoparticles were adsorbed on the rock surface to form spherical particle aggregates. The attached HMN altered the structure and roughness of the rock surface, resulting in a transformation of the surface wettability. In addition, the pores on the shale surface were sealed due to the adsorption of nanoparticles, which prevented water from entering the shale interior causing hydration (Ni et al., 2019b).

AFM was also used to study the changes of shale surface

morphology before and after HMN treatment. Fig. 10 shows the AFM images of the shale before and after the 2.0 wt% HMN treatment. The uneven surface, as well as many depressions on the original shale, indicated the heterogeneity of its surface, as shown in Fig. 10a and c. Fig. 10b and d show that the surface of the HMN-treated shale was flatter and more homogeneous, which was attributed to the adsorption of HMN on the surface. The SEM results were consistent with the AFM measurements.

3.4.2. FTIR analysis

The changes of the chemical structure of the shale surface before and after HMN adsorption are shown in Fig. 11. For the FTIR spectrum of untreated shale, the insignificant absorption peak at 3587 cm⁻¹ was a stretching vibration peak of the hydroxyl group (the structural water) of the clay mineral in shale. The apparent absorption peak at 1429 cm^{-1} was caused by the CO_3^{2-} asymmetric stretching vibrations of silicate minerals (such as calcite) in the shale (Chen et al., 2014). The absorption band at 1008 cm⁻¹ originated from the Si-O stretching vibration and was attributed to silicate minerals such as quartz and illite in the shale. The two absorption peaks at 795 and 458 cm⁻¹ in the fingerprint region corresponded to the Si-O-Si stretching vibration and Si-O bending vibration of silicate minerals, respectively (Kim et al., 2009). It was notable that the absorption peaks at a given location may be generated by multiple minerals overlapping in the absorbance region. For the FTIR spectrum of shale treated with 2.0 wt% HMN, the stretching vibrational peak of the -OH shifted towards the lower wavenumber after the adsorption of HMN on the shale surface. A strong absorption peak was found at 3441 cm^{-1} . Moreover, the two absorption bands were found at 2919 and 2850 cm^{-1} , which were the stretching vibrations of the $-CH_2$ and -CH₃ of the surfactant component in HMN, respectively (Ma et al., 2010). Besides, the Si-O antisymmetric stretching vibration peak found at $1113 \ cm^{-1}$ was one of the characteristic peaks of silica nanoparticles. The phenomenon further demonstrated the successful adsorption of HMN on the shale surface.

3.4.3. Wettability measurements

One of the root causes of wellbore instability is the reduction in the strength of the shale due to WBDF filtrate intrusion. The water contact angles of shale aged at 90 °C for 16 h in WBDFs of Xinjiang Oilfield with different HMN concentrations are shown in Fig. 12. Fig. 12a shows that the contact angle of the shale in the HMN-free WBDFs of Xinjiang Oilfield was only 25°, indicating its high hydrophilicity. In contrast, the contact angle of shale increased with HMN concentrations. In detail, the contact angle of the shale was increased to 42° owing to the addition of 1.0 wt% HMN to the WBDFs, as shown in Fig. 12b. Furthermore, the contact angle of the shale was improved to 82° after adding 2.0 wt% HMN (Fig. 12c) and reached wetting reversal with a 3.0 wt% addition (Fig. 12d). The result indicated a significant increase in the hydrophobicity of the shale and less interaction with water. In this way, shale hydration swelling and dispersion were fundamentally inhibited through wettability alteration (Ni et al., 2019).

3.4.4. Glass capillary tube rise tests

Glass capillary tube rise tests were used to simulate water entering the shale interior under the capillary force. Fig. 13 shows the rise height of water in glass capillary tubes treated with different solutions (water, 1.0 wt% HMN, 2.0 wt% HMN, 3.0 wt% HMN) at 90 °C for 16 h. The rise height in the water-treated capillary tube was the highest, reaching 2.9 cm. The phenomenon indicated that the capillary tube was water-wetted, and the capillary force was the driving force for water to enter the capillary tube. Shale is a non-homogeneous rock rich in microporosity. When the

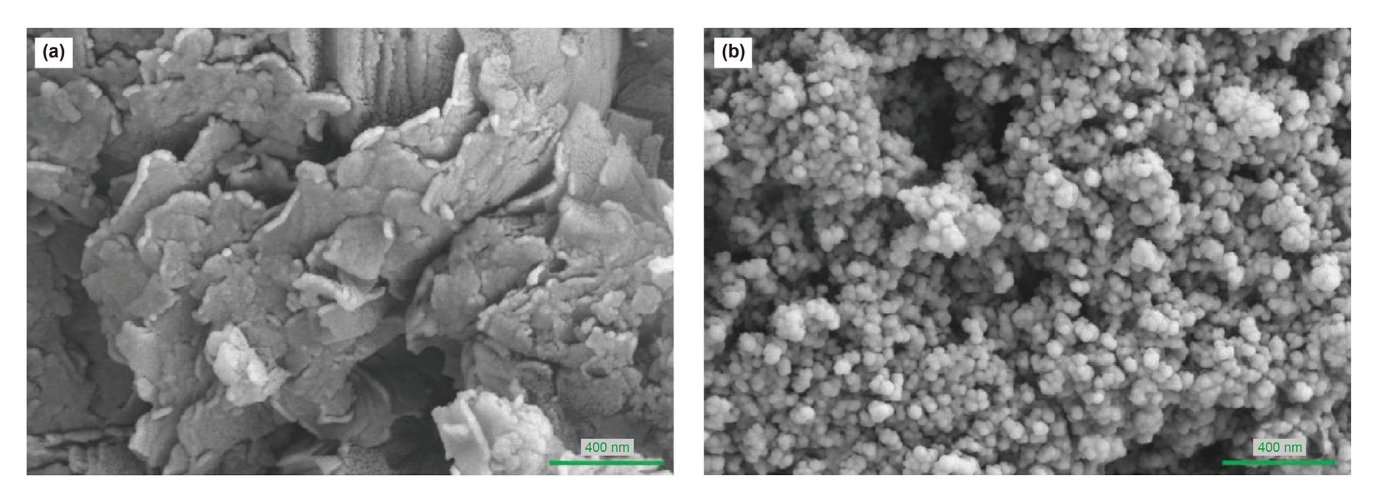


Fig. 9. SEM images of shale without treatment (a) and treated with 2.0 wt% HMN (b).

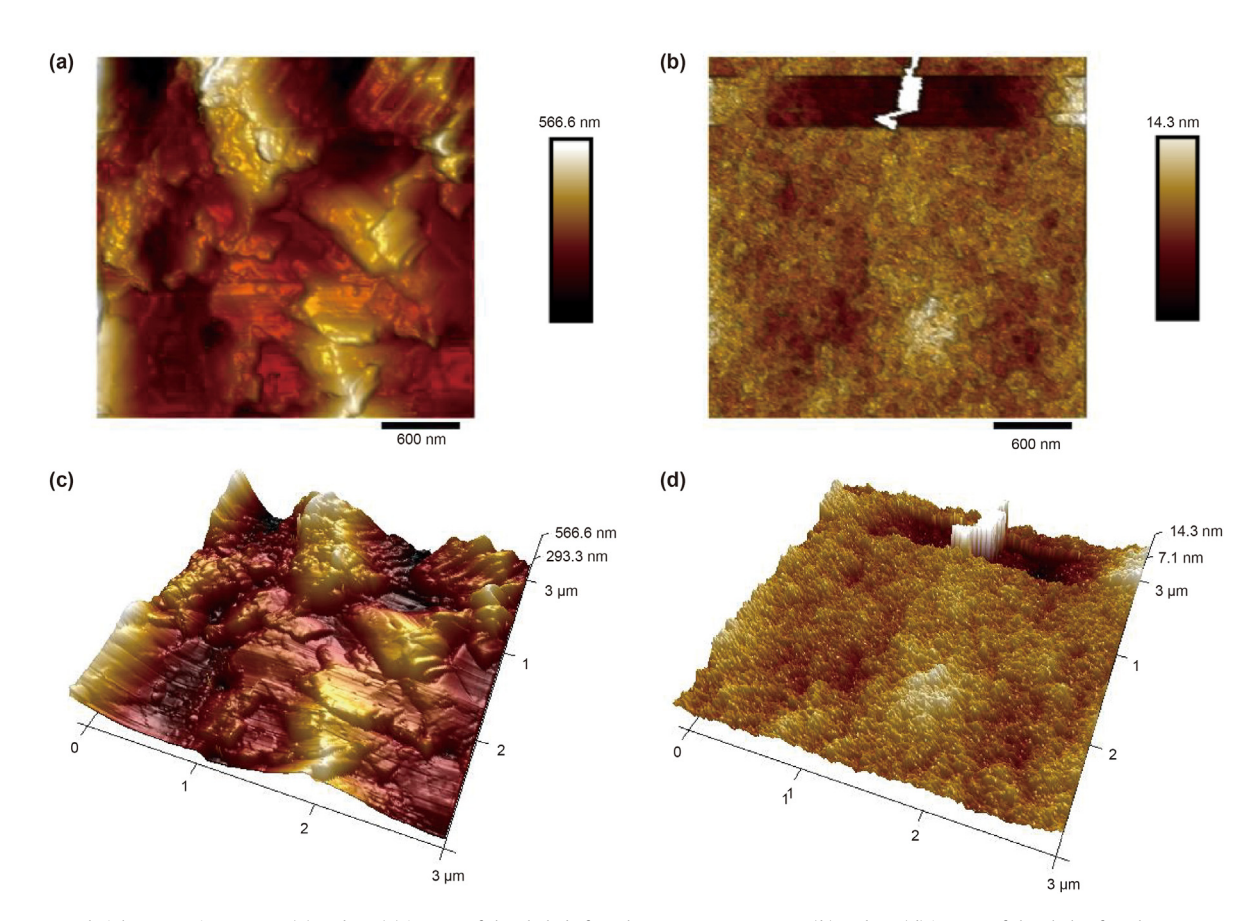


Fig. 10. AFM height sensor images. 2D (a) and 3D (c) images of the shale before the HMN treatment, 2D (b) and 3D (d) images of the shale after the HMN treatment.

rock is hydrophilic, water is drawn into the shale interior driven by capillary forces, resulting in shale hydration. For the HMN-treated capillary tubes, the rise height decreased with increasing HMN concentration, as shown in Fig. 13. After treating the capillary tube with 1.0 wt% HMN, the rise height was 0.3 cm, and the rise height was below the liquid level (-0.9 cm) at 3.0 wt% concentration. The phenomenon demonstrated that the capillary force converted from the driving force of water entry to the resistance after HMN adsorption. It was a transformation that effectively reduced the instability caused by the hydration of the shale.

The mechanism of HMN to enhance wellbore stability is shown in Fig. 14. According to the previous discussion, the action mechanism of HMN was as follows. Before the HMN adsorption, the shale surface was hydrophilic, which led to a reduction in strength. HMN was adsorbed on the negatively charged shale surface under the effect of electrostatic attraction. After HMN adsorption, hydrophobic structures containing multiple hydrophobic hydrocarbon chains were formed on the shale surface to induce wetting inversion. The transformation of rock surface wettability produced a repulsive effect of the shale to the water to reduce shale hydration.

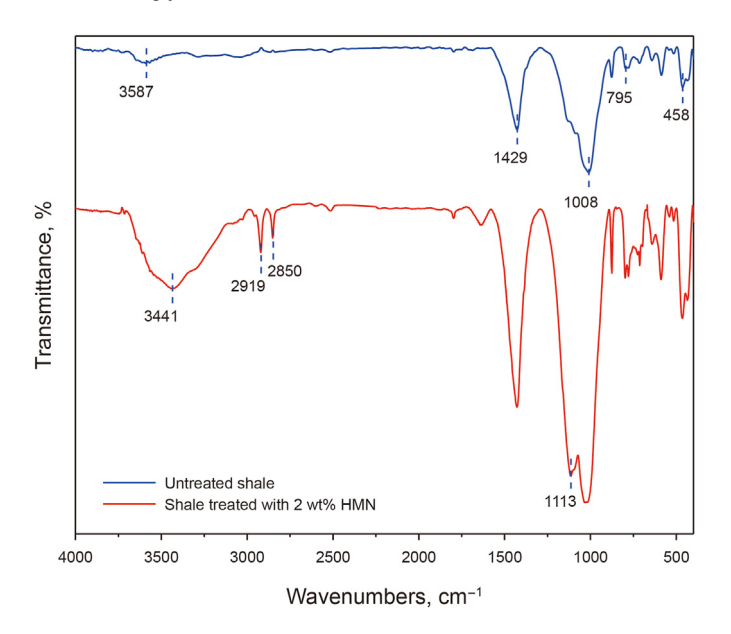


Fig. 11. FTIR spectra of shale before and after 2.0 wt% HMN treatment.

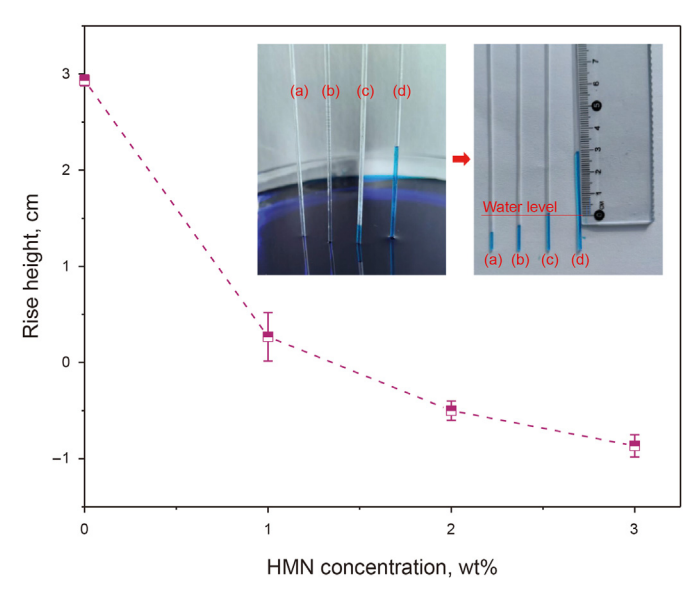


Fig. 13. The rise height of water in the glass capillary tubes treated with different HMN concentrations: (**a**) 3.0 wt%; (**b**) 2.0 wt%; (**c**) 1.0 wt%; (**d**) 0 (treated with water).

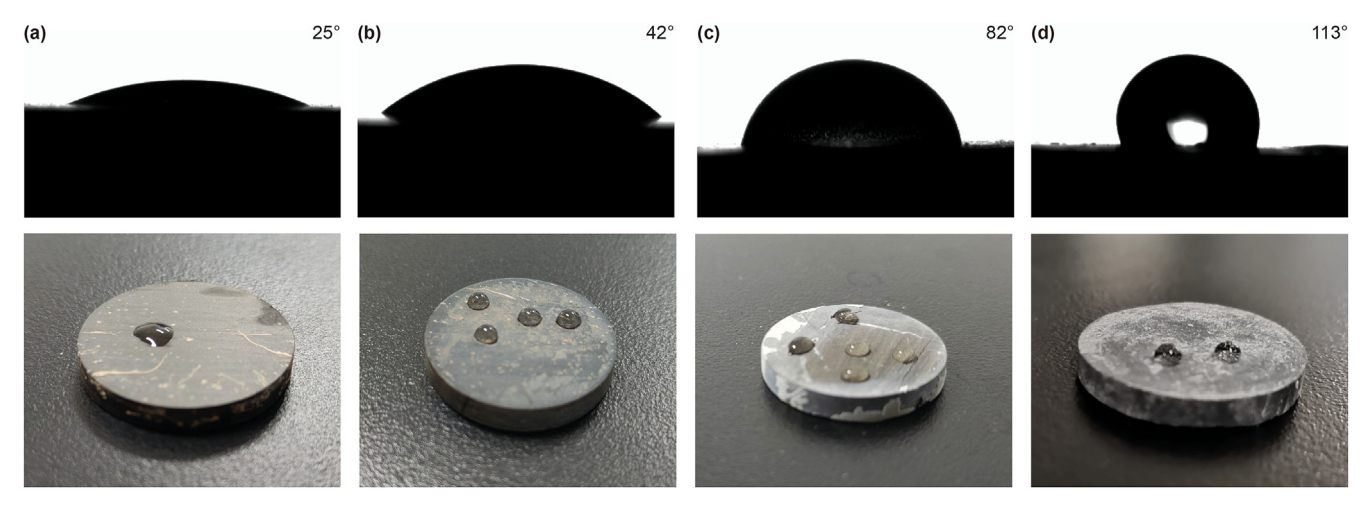


Fig. 12. Water contact angle of shale aged at 90 °C for 16 h in WBDFs of the Xinjiang Oilfield containing different HMN contents: (a) HMN-free; (b) 1.0 wt%; (c) 2.0 wt%; (d) 3.0 wt%.

In addition, HMN sealed the pores of the shale, which prevented water from entering the interior of the shale and reduced hydration.

4. Conclusions

In this work, hydrophobically modified nanoparticles (HMN) were synthesized to enhance the performance of WBDFs in the Xinjiang Oilfield, especially for stabilizing the wellbore performance. The enhancing effects of HMN on comprehensive performance of WBDFs in the Xinjiang Oilfield, including inhibition performance, plugging performance, and lubrication performance, were confirmed by experimental results. Furthermore, the improvement effect of HMN on wellbore stability was evaluated by compressive strength test. The action mechanism of HMN was proposed based on experimental results. However, since illite-rich rock samples were used in this study, the conclusions of this study may not be applicable to other rock samples. Several specific conclusions from the results were as follows:

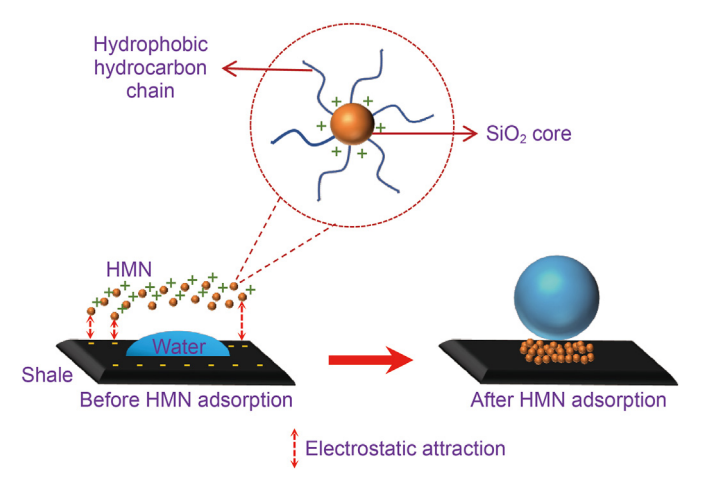


Fig. 14. Mechanism analysis of HMN.

- (1) HMN could significantly improve the inhibition performance of WBDFs in the Xinjiang Oilfield. The linear swelling of clay was reduced by 71.4%, and the recovery of shale cuttings was increased to more than 80 wt% with 3.0 wt% HMN.
- (2) HMN also enhanced the plugging and lubrication performance of WBDFs in the Xinjiang Oilfield to some extent and has less influence on the rheology and filtration loss performance of drilling fluids.
- (3) The addition of HMN to WBDFs of the Xinjiang Oilfield considerably prevented the decline of shale strength.
- (4) Shale surface wettability was altered with HMN, which resulted in the reversal of capillary forces and reduced shalewater interactions to inhibit shale hydration.

Acknowledgments

The authors are thankful to the National Natural Science Foundation of China (51904329, 52174014), the Major Scientific and Technological Projects of CNPC (ZD 2019-183-005), and Key R & D Program of Shandong Province (No.2020ZLYS07).

References

- Al-Anssari, S., Barifcani, A., Wang, S., Maxim, L., Iglauer, S., 2016. Wettability alteration of oil-wet carbonate by silica nanofluid. J. Colloid Interface Sci. 461, 435–442. https://doi.org/10.1016/j.jcis.2015.09.051.
- Bai, X., Wang, H., Luo, Y., Zheng, X., Zhang, X., Zhou, S., et al., 2017. The structure and application of amine-terminated hyperbranched polymer shale inhibitor for water-based drilling fluid. J. Appl. Polym. Sci. 134, 45466. https://doi.org/ 10.1002/app.45466.
- Cai, J., Chenevert, M.E., Sharma, M.M., Friedheim, J., 2012. Decreasing water invasion into Atoka shale using nonmodified silica nanoparticles. SPE Drill. Complet. 27 (1), 103–112. https://doi.org/10.2118/146979-MS.
- Chen, Y., Furmann, A., Mastalerz, M., Schimmelmann, A., 2014. Quantitative analysis of shales by KBr-FTIR and micro-FTIR. Fuel 116, 538–549. https://doi.org/10.1016/j.fuel.2013.08.052.
- Chu, Q., Lin, L., Su, J., 2020. Amidocyanogen silanol as a high-temperature-resistant shale inhibitor in water-based drilling fluid. Appl. Clay Sci. 184, 105396. https://doi.org/10.1016/j.clay.2019.105396.
- Davarpanah, A., Mirshekari, B., 2019. Effect of formate fluids on the shale stabilization of shale layers. Energy Rep. 5, 987–992. https://doi.org/10.1016/j.egyr.2019.07.016.
- Feng, C., Kong, Y., Jiang, G., Yang, J., Pu, C., Zhang, Y., 2012. Wettability modification of rock cores by fluorinated copolymer emulsion for the enhancement of gas and oil recovery. Appl. Surf. Sci. 258 (18), 7075–7081. https://doi.org/10.1016/ j.apsusc.2012.03.180.
- Gao, C.H., 2019. A survey of field experiences with formate drilling fluid. SPE Drill. Complet. 34 (4), 450–457. https://doi.org/10.2118/195699-PA.
- Gholami, R., Elochukwu, H., Fakhari, N., Sarmadivaleh, M., 2018. A review on borehole instability in active shale formations: interactions, mechanisms and inhibitors. Earth Sci. Rev. 177, 2–13. https://doi.org/10.1016/ J.EARSCIREV.2017.11.002.
- Guancheng, J., Yourong, Q., Yuxiu, A., Xianbin, H., Yanjun, R., 2016. Polyethyleneimine as shale inhibitor in drilling fluid. Appl. Clay Sci. 127–128, 70–77. https://doi.org/10.1016/J.CLAY.2016.04.013.
- Huang, X.B., Sun, J.S., Huang, Y., Yan, B.C., Dong, X.D., Liu, F., et al., 2021. Laponite: a

- promising nanomaterial to formulate high-performance water-based drilling fluids. Petrol. Sci. 18 (2), 579–590. https://doi.org/10.1007/s12182-020-00516-z.
- Ibrahim, M.A., Saleh, T.A., 2020. Partially aminated acrylic acid grafted activated carbon as inexpensive shale hydration inhibitor. Carbohydr. Res. 491, 107960. https://doi.org/10.1016/j.carres.2020.107960.
- Jiang, G., Zhang, X., Dong, T., Xuan, Y., Wang, L., Jiang, Q., 2018. A new inhibitor of P(AM-DMDAAC)/PVA intermacromolecular complex for shale in drilling fluids. J. Appl. Polym. Sci. 135 (1), 1–8. https://doi.org/10.1002/app.45584.
- Kim, J.M., Chang, S.M., Kong, S.M., Kim, K.S., Kim, J., Kim, W.S., 2009. Control of hydroxyl group content in silica particle synthesized by the sol-precipitation process. Ceram. Int. 35 (3), 1015–1019. https://doi.org/10.1016/ j.ceramint.2008.04.011.
- Lei, M., Huang, W., Sun, J., Shao, Z., Wu, T., Liu, J., et al., 2020. Synthesis of car-boxymethyl chitosan as an eco-friendly amphoteric shale inhibitor in water-based drilling fluid and an assessment of its inhibition mechanism. Appl. Clay Sci. 193, 105637. https://doi.org/10.1016/j.clay.2020.105637.
- Ma, X.K., Lee, N.H., Oh, H.J., Kim, J.W., Rhee, C.K., Park, K.S., et al., 2010. Surface modification and characterization of highly dispersed silica nanoparticles by a cationic surfactant. Colloid. Surf. A Physicochem. 358 (1–3), 172–176. https:// doi.org/10.1016/j.colsurfa.2010.01.051.
- Ma, F., Pu, X., Wang, B., Li, J., Cao, C., 2017. Preparation and evaluation of polyampholyte inhibitor DAM. RSC Adv. 7 (78), 49320–49328. https://doi.org/10.1039/c7ra08385h.
- Ni, X., Jiang, G., Li, Y., Yang, L., Li, W., Wang, K., et al., 2019. Synthesis of superhydrophobic nanofluids as shale inhibitor and study of the inhibition mechanism. Appl. Surf. Sci. 484, 957–965. https://doi.org/10.1016/j.apsusc.2019.04.167.
- Parizad, A., Shahbazi, K., 2016. Experimental investigation of the effects of SnO₂ nanoparticles and KCl salt on a water base drilling fluid properties. Can. J. Chem. Eng. 94 (10), 1924—1938. https://doi.org/10.1002/cjce.22575.
- Peng, B., Luo, P.Y., Guo, W.Y., et al., 2013. Structure-property relationship of polyetheramines as clay-swelling inhibitors in water-based drilling fluids. J. Appl. Polym. Sci. 129 (3), 1074–1079. https://doi.org/10.1002/app.38784, 1074-1079. Rivet, S.M., 2009. Coreflooding Oil Displacements with Low Salinity Brine.
- Saffari, H.R.M., Soltani, R., Alaei, M., Soleymani, M., 2018. Tribological properties of water-based drilling fluids with borate nanoparticles as lubricant additives. J. Pet. Sci. Eng. 171, 253—259. https://doi.org/10.1016/j.petrol.2018.07.049, 171 253-259
- Saleh, T.A., Ibrahim, M.A., 2019. Advances in functionalized Nanoparticles based drilling inhibitors for oil production. Energy Rep. 5, 1293—1304. https://doi.org/ 10.1016/j.egyr.2019.06.002.
- Sheshdeh, M.J., 2015. A review study of wettability alteration methods with regard to nano-materials application. In: SPE Bergen One Day Seminar. Society of Petroleum Engineers. https://doi.org/10.2118/173884-MS.
- Suter, J.L., Coveney, P.V., Anderson, R.L., Greenwell, H.C., Cliffe, S., 2011. Rule based design of clay-swelling inhibitors. Energy Environ. Sci. 4 (11), 4572–4586. https://doi.org/10.1039/c1ee01280k.
- Yang, X., Shang, Z., Liu, H., Cai, J., Jiang, G., 2017. Environmental-friendly salt water mud with nano-SiO₂ in horizontal drilling for shale gas. J. Pet. Sci. Eng. 156, 408–418. https://doi.org/10.1016/J.PETROL.2017.06.022.
- Young, D.A., Smith, D.E., 2000. Simulations of clay mineral swelling and hydration: dependence upon interlayer ion size and charge. J. Phys. Chem. B 104 (39), 9163–9170. https://doi.org/10.1021/jp000146k.
- Yue, Y., Chen, S., Wang, Z., Yang, X., Peng, Y., Cai, J., et al., 2018. Improving wellbore stability of shale by adjusting its wettability. J. Pet. Sci. Eng. 161, 692–702. https://doi.org/10.1016/j.petrol.2017.12.023.
- Zhong, H., Qiu, Z., Sun, D., Zhang, D., Huang, W., 2015. Inhibitive properties comparison of different polyetheramines in water-based drilling fluid. J. Nat. Gas Sci. Eng. 26, 99–107. https://doi.org/10.1016/j.jngse.2015.05.029.
- Zhong, H., Qiu, Z., Tang, Z., Zhang, X., Xu, J., Huang, W., 2016. Study of 4, 4'-methylenebis-cyclohexanamine as a high temperature-resistant shale inhibitor. J. Mater. Sci. 51 (16), 7585–7597.